MAPPING CHARON AT 2.21 MICRONS J. C. Cook[1], C. M. Dalle Ore[2,3], R. P. Binzel[4], D. P. Cruikshank[2], A. Earle[4], K. Ennico[2], W. M. Grundy[5], C. Howett[6], D. J. Jennings[7], A. W. Lunsford[7], C. B. Olkin[6], A. H. Parker[6], S. Philippe[8], S. Protopapa[9], D. Reuter[7], B. Schmitt[8], J. A. Stansberry[10], S. A. Stern[6], A. Verbiscer[11], H. A. Weaver[12], L. A. Young[6], the New Horizons Surface Composition Theme Team, and the Ralph Instrument Team, [1]Pinhead Institute, Telluride, CO, [2]NASA Ames Research Center, Moffat Field, CA, [3]SETI Institute, Mountain View, CA, [4]Massachusetts Institute of Technology, Cambridge, MA, [5]Lowell Observatory, Flagstaff, AZ, [6]Southwest Research Institute, Boulder, CO, [7]NASA Goddard Space Flight Center, Greenbelt, MD, [8]Institut de Planétologie et Astrophysique de Grenoble, Grenoble, France, [9]University of Maryland, College Park, MD, [10]Space Telescope Science Institute, Baltimore, MD, [11]University of Virginia, Charlottesville, VA, [12]John Hopkins University, Applied Physics Laboratory, Laurel, MD. (jasoncampbellcook@gmail.com)

Introduction: Before the *New Horizons* flyby of the Pluto-system on July 14, 2015, we understood Charon's surface to be a mixture of crystalline H_2O-ice and NH_3-hydrate. Mutual events of Pluto and Charon in the mid-to-late 1980s showed us that the surface of Charon is largely covered by H_2O-ice [1]. It was later revealed to be in the crystalline phase alongside evidence for an absorption band around 2.21 μm, possibly due to NH_3-hydrate [2, 3, 4]. Work by [5, 6, 7] showed that the band was undoubtedly present. [8] showed the 2.21 μm band position shifts with longitude.

Observations: Using the Ralph [9] instrument, *New Horizons* successfully obtained images and spectra of Charon. Ralph is a dual channel instrument with MVIC (Multi-spectral Visible Imaging Camera), the visible color imager, and LEISA (Linear Etalon Imaging Spectral Array), the near infrared spectrograph. LEISA covers the spectral range 1.25 to 2.50 μm at a resolving power ($\lambda/\Delta\lambda$) of 240, and 2.10 to 2.25 μm at a resolving power of 560. We examined three LEISA scans of Charon taken a few hours before closet approach. These scans were at a distance of 483,000, 136,000 and 81,000 km, giving spatial scales of 30, 9 and 5 km/pixel.

Methodology: In addition to the standard LEISA pipeline to flat field and flag bad pixels, our analysis includes steps for cleaning and re-flattening. The cleaning steps are performed in order to remove an electronic noise pattern that changes in each LEISA frame. We take advantage of the fact that the pattern repeats in each quadrant of the frame. By masking out the target and median stacking each quadrant we produce a fairly reliable estimate of the background noise pattern.

We use three Charon scans to provide improvements to the flat field by obtaining the median signal at each native LEISA pixel while Charon passes through that pixel. This essentially averages over spatial variations. Brightness variations over a single row (wavelength) are then removed by fitting a second order polynomial. closest to Charon nearly fills the field

After the data are cleaned and flattened, we remove motion distortion. Thrusters may be fired during the scan if the target reaches a deadband. We use the known spacecraft trajectory to correct for its motion. Finally, we build a cube. This step does not resample the data, it just reorders the pixels such that each plane of the cube is a single wavelength. We later rebin the data to decrease computation time and boost signal-to-noise. The rebinning factor is different for each scan.

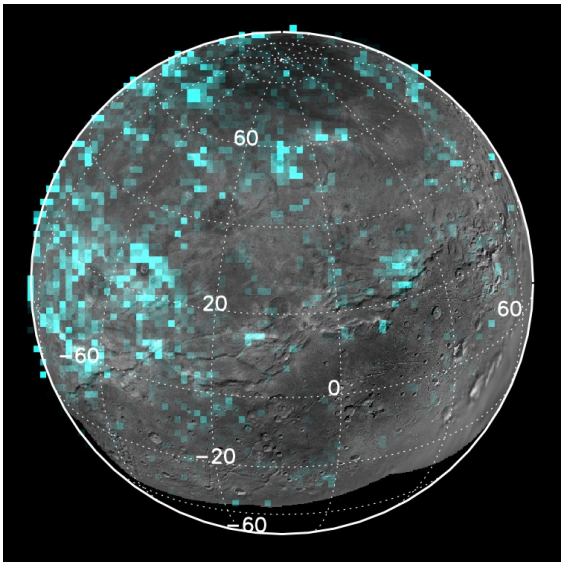

Figure 1: Composite image of Charon basemap and residual map at 2.21 μm. Blue pixels correspond to regions with greater absorption at 2.21 μm. North is up, and east is to the right.

Once the cube is built and rebinned, we perform Hapke modeling of each spectrum. We assume a simple model with an intimate mixture of amorphous H_2O-ice [10], crystalline H_2O-ice [11] in three size ranges, a Triton tholin [12] and Pluto tholin [13, 14]. All water ice is assumed to be 50 K. Subtracting the model spectrum from the observations yields the the residual spectrum.

Results: Shown in Fig. 1 is a composite image of the Charon basemap (grayscale) and the residual map of Charon at 2.21 μm. Regions of greater absorption are colored blue. This map shows that there are several $>$50 km regions on Charon's surface which have absorption at 2.21 μm. The basemap shows that these regions are highly correlated with the bright rays around craters, but not the dark material within the craters.

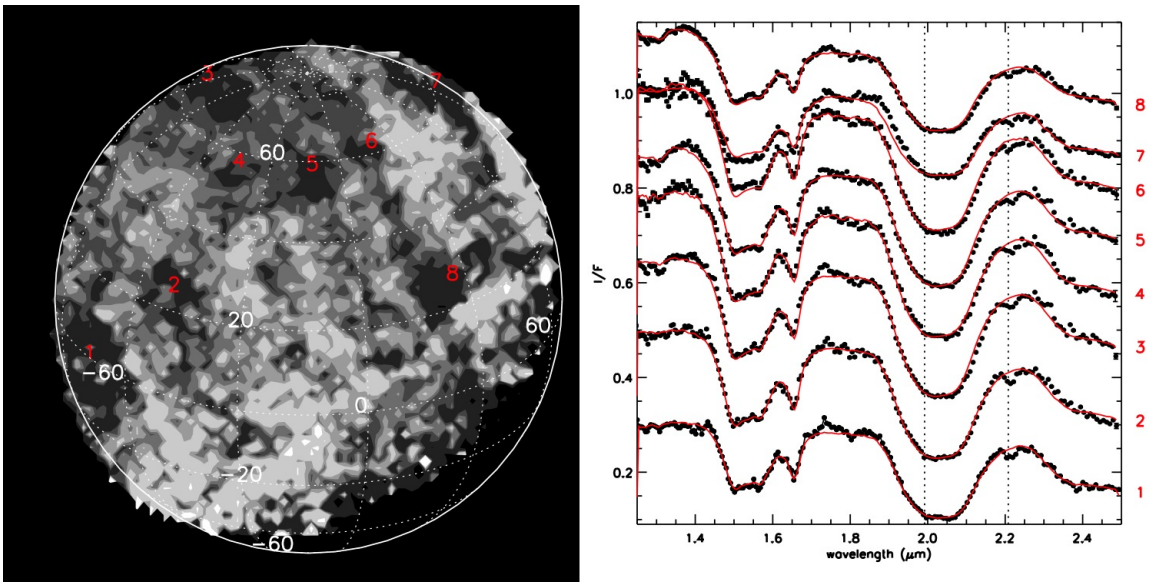

Figure 2: Contour map of Charon at 2.21 μm and associated spectra. We label regions 1-8 on the map and show the spectrum from each region on the right. The average Hapke spectral model is also shown in red. Each spectrum is labeled with the corresponding region from the contour map. Two vertical dashed lines are shown at 2.208 and 1.992 μm, the measured position for NH_3-H_2O-ice mixtures with <2.5% NH_3 [15].

In Fig. 2, we show the residual map as a series of contour levels. Each contour level contains 20% of the data. We label 8 distinct regions (1-8) in the contour map and show the associated spectra on the right side. The spectra are shown with average Hapke spectral models in red. The models highlight the deviation near 2.21 μm.

Discussion & Conclusion: NH_3-hydrates and NH_3-H_2O-ice mixtures have two identifiable bands in our spectral range. We have focused on the 2.21 μm for this work, but a another narrow band appears around 1.99 μm. The exact position of each band can change with concentration [15], shifting to longer wavelengths as the NH_3 fraction increases. The relative strengths of the two bands are similar, thus the detection of the 2.21 μm band should also yield a band near 1.99 μm. This second band has never been seen in ground based spectroscopy, possibly due to nearby telluric contamination. But our analysis also shows little absorption near 1.99 μm, although it may be present in some of the spectra we show (regions 1 and 2), it is not nearly as strong as anticipated based on laboratory spectra.

Recent work by [16] showed a slightly different distribution to NH_3. That work was based on clustering of the 2.0 μm band of H_2O-ice. Their work showed the surface can be characterized by three spectral types with minor variations among them. The region that corresponded to the highest concentration of NH_3-hydrate is associated with regions of high albedo (*e.g.,* bright crater rays), large grains H_2O-ice and neutral slope/least amount of Pluto tholins. They suggested that the reason for the differences may be due to different forms of NH_3, one which is associated with the 1.99 μm band and the other with the 2.21 μm. band.

These somewhat differing results suggest something more than NH_3-H_2O-ice mixtures may be present on Charon. Ammonium, NH_4, may be the a likely candidate. It has a spectrum that is similar to NH_3-hydrates, but lacks the band at 1.99 μm [17]. The recent detection of ammoniated clays on Ceres by Dawn [18] shows the various forms NH_3 has the potential to take.

References: [1] Buie, M. W., et al. (1987) *Nature* 329:522. [2] Buie, M. W., et al. (2000) *Icarus* 148:324. [3] Brown, M. E., et al. (2000) *Science* 287:107. [4] Dumas, C., et al. (2001) *Astron. J.* 121:1163. [5] Cook, J. C., et al. (2007) *ApJ* 663:1406. [6] Verbiscer, A. J., et al. (2007) vol. 38 of *Lunar and Planetary Science Conference* 2318. [7] Merlin, F., et al. (2010) *Icarus* 210:930. [8] DeMeo, F. E., et al. (2015) *Icarus* 246:213. [9] Reuter, D. C., et al. (2008) *Space Sci. Rev.* 140:129.arXiv:0709.4281. [10] Mastrapa, R. M., et al. (2008) *Icarus* 197:307. [11] Grundy, W. M., et al. (1998) *J. Geophys. Rev.* 103:25809. [12] Khare, B. N., et al. (1994) vol. 26 of *Bulletin of the American Astronomical Society* 1176. [13] Materese, C. K., et al. (2015) *ApJ* 812:150. [14] Cruikshank, D. P., et al. (2016) vol. 47 of *Lunar and Planetary Science Conference* 1700. [15] Zheng, W., et al. (2008) *ApJ* 674:1242-1250. [16] Dalle Ore, C. M., et al. (2017) *Icarus*. [17] Moore, M. H., et al. (2007) *Icarus* 190:260. [18] de Sanctis, M. C., et al. (2015) *Nature* 528:241.